

Absolute cross sections for the $^{58,60}\text{Ni}(^{16}\text{O}, X)$ reactions

R. L. Robinson, H. J. Kim, and J. L. C. Ford, Jr.
Oak Ridge National Laboratory, Oak Ridge, Tennessee 37830*
 (Received 27 August 1973)

The absolute cross sections for a variety of reactions resulting from bombardment of $^{58,60}\text{Ni}$ with 38-, 42-, and 46-MeV ^{16}O ions were determined from yields of γ rays observed from the decay of resulting radioactivities and from yields of in-beam γ rays. The strongest reactions are $(^{16}\text{O}, pm)$, $(^{16}\text{O}, 2p)$, and $(^{16}\text{O}, \alpha p)$. Other identified reactions are $(^{16}\text{O}, p)$, $(^{16}\text{O}, 2n)$, $(^{16}\text{O}, \alpha)$, $(^{16}\text{O}, \alpha n)$, $(^{16}\text{O}, 2\alpha)$, $(^{16}\text{O}, 2pm)$, $(^{16}\text{O}, 3p)$, $(^{16}\text{O}, ^{12}\text{C})$, and $(^{16}\text{O}, ^{15}\text{N})$. At the higher projectile energies the total cross sections are in reasonable agreement with the reaction cross sections based on an optical-model calculation. The relative yields of the reaction products were compared to predictions for statistical decay of a compound-nuclear system by neutron, proton, and α -particle emission. This model does account for the general features of the experimental data; in particular it correctly predicts that charged-particle emission strongly competes with neutron emission.

<p>NUCLEAR REACTIONS $^{58,60}\text{Ni}(^{16}\text{O}, X)$, $E_{^{16}\text{O}} = 38, 42, 46$ MeV; measured E_γ, I_γ; deduced $\sigma(E)$.</p> <p>RADIOACTIVITY ^{74}Br; measured E_γ, I_γ, $T_{1/2}$.</p>

I. INTRODUCTION

One of the most promising uses of heavy-ion projectiles is in inducing reactions which produce nuclei far from the valley of stability. Even though this technique is being increasingly applied to production of new and scantily studied neutron-deficient nuclei, little quantitative information exists on the cross sections for the various reaction products and, in particular, on how far from stability nuclei can be produced in observable quantities. The latter is equivalent to asking what is the competition between reactions in which neutrons are emitted, i.e., reactions that lead to nuclei away from stability, and in which charged particles are emitted.¹

It is generally assumed that heavy-ion-induced reactions are predominantly compound (Ref. 2 gives an excellent review of this process), and thus, in principle, the relative magnitude of the various reactions can be calculated. An extensive effort to do so has been carried out by Blann³ who considered the statistical decay via neutron, proton, and α -particle emission of the compound system and of the resulting nuclei. His calculations give discouragingly small cross sections for production of nuclei well away from stability, e.g., the peak cross section of the $^{58}\text{Ni}(^{16}\text{O}, 5n)^{69}\text{Kr}$ reaction is predicted to be 20×10^{-6} mb. But there are many uncertainties in these types of complex calculations: What is the spin distribution of the states formed in the compound-nuclear system? What is the dependence of the level density on spin and yrast level on energy? Emission of what kinds

of particles from the compound system need to be considered? What is the competition between particle and γ -ray emission? How important is preequilibrium decay?

We have initiated a program to provide experimental data that can be used to check the validity of such calculations and guide toward improved versions whereby cross-section predictions for producing nuclei far from stability can be carried out with greater confidence. Specifically our approach is to determine for heavy-ion-induced reactions, the absolute cross sections for as many reaction products as possible and has been applied in the present study to the $^{16}\text{O} + ^{58,60}\text{Ni}$ reactions. These cross sections were deduced principally from the yields of γ rays from the residual radioactivities. Because of the high resolution of a Ge(Li) detector many products can be identified simultaneously from the γ -ray energies and intensities and from the half-lives of the radioactivities. There are several factors which influence the effectiveness of this technique: the half-life of the radioactivity, the relative decay of the activity to excited states and the ground state, and prior knowledge of the decay properties of the activity. Although performing chemical separation of the products would allow detection of reactions with even smaller cross sections, it has the disadvantages of making absolute cross-section determinations more difficult and of requiring a new target for each irradiation.

In cases where the products were stable, in-beam γ -ray spectroscopy was employed to supplement the radioactivity studies. However, in-

beam studies are more limited in usefulness since, besides having one less signature for identification, i.e., the half-life, there is still little known about the levels populated by particle emission following heavy-ion-induced reactions.

Absolute cross sections for $^{58,60}\text{Ni}(^{16}\text{O}, X)$ reactions for $E_{^{16}\text{O}} = 38, 42,$ and 46 MeV have been determined.⁴ Although the principal interest is the cross sections for few-nucleon emission, we for completeness also looked for γ rays from nuclei resulting from one- and two-particle transfer. The total reaction cross section is compared to predictions of an optical model; the relative production of the residual nuclei is compared to that given by the statistical decay of a compound nucleus. In addition, some new results were obtained about the decays of ^{72}Br and ^{74}Br . Those for ^{74}Br are presented in Appendix B. Because so little was known about the decay of ^{72}Br , it was also studied via γ - γ coincidences and the findings are reported in a separate publication.⁵

Some compound-nuclear calculations for $^{58}\text{Ni} + ^{16}\text{O}$ and $^{60}\text{Ni} + ^{16}\text{O}$ systems already exist in the literature. Doron and Blann⁶ presented the relative probability for decay of compound systems formed with targets in the mass range $69 \leq A \leq 88$, and ^{16}O and ^{32}S projectiles. This broad survey also included the relative experimental cross sections obtained for the reactions $^{58}\text{Ni}(^{16}\text{O}, \alpha p)$, $(^{16}\text{O}, 2p n)$, $(^{16}\text{O}, pn)$, and $^{60}\text{Ni}(^{16}\text{O}, \alpha n)$ and $(^{16}\text{O}, pn)$. Nolte *et al.*⁷ have also reported relative cross sections for exit channels in which two nucleons are emitted in the $^{58,60}\text{Ni} + ^{16}\text{O}$ reactions.

II. EXPERIMENTAL PROCEDURE

Targets of $^{58,60}\text{Ni}$ were irradiated with 38-, 42-, and 46-MeV ^{16}O projectiles extracted from the Oak Ridge National Laboratory (ORNL) tandem Van de Graaff accelerator. The thickness of the targets, which were enriched to about 99%, was 1.00 mg/cm^2 for ^{58}Ni and 1.64 mg/cm^2 for ^{60}Ni . Recoil products were stopped in a 7-mg/cm^2 gold foil placed immediately behind the target.

Figure 1 illustrates schematically the experimental setup employed for multiple irradiations. After each irradiation of a predetermined length set by the timer scaler associated with the controller, the target was swung to the detector position, the beam was stopped (to reduce background), and the analyzer was started. γ rays were detected with a large Ge(Li) semiconductor and recorded in several 2048-channel groups of the analyzer (generally 7 groups) as a function of time determined by a second timer scaler. At the end of a time equal to the bombarding time, the target was returned to the beam position, the beam was "turned on," and the cycle was repeated. This scheme can be used to study activities with half-lives of about a second or more. For long irradiations (more than an hour) the target was removed from the chamber after irradiation and taken to a lower background area for the γ -ray studies.

To determine absolute cross sections, it is important that a careful history be kept of the beam current. This was done with a second analyzer

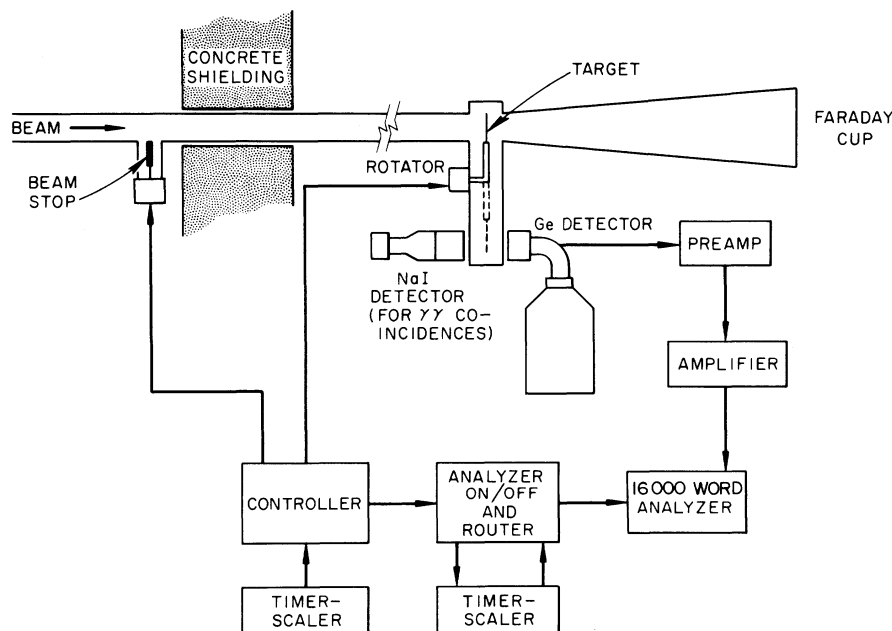


FIG. 1. Schematic of the experimental apparatus.

which stored current-integrator pulses as a function of time.

Identification of the γ rays in the radioactive products was based on their energies and relative intensities, and on the half-lives associated with their decay. The latter were extracted from the sequential spectra taken after each irradiation.

In order to observe a change of yield during the detection period for products with appreciably different half-lives, several runs of different detection-irradiation periods were carried out. Specifically, the irradiation times for ^{58}Ni were 400 sec, 1000 sec, and 4.1 h; for ^{60}Ni they were 80 sec, 1000 sec, 2600 sec, 4000 sec, and 4.9 h. This variety was also useful in that the relative experimental sensitivity to the products of different half-lives was dependent on the different periods as illustrated in Fig. 2 by several hypothetical examples. The curves show the decays that take place during all detection periods if the production rate is taken as one radioactive nucleus per sec. The irradiation and detection times, which are equal, for each cycle are specified on

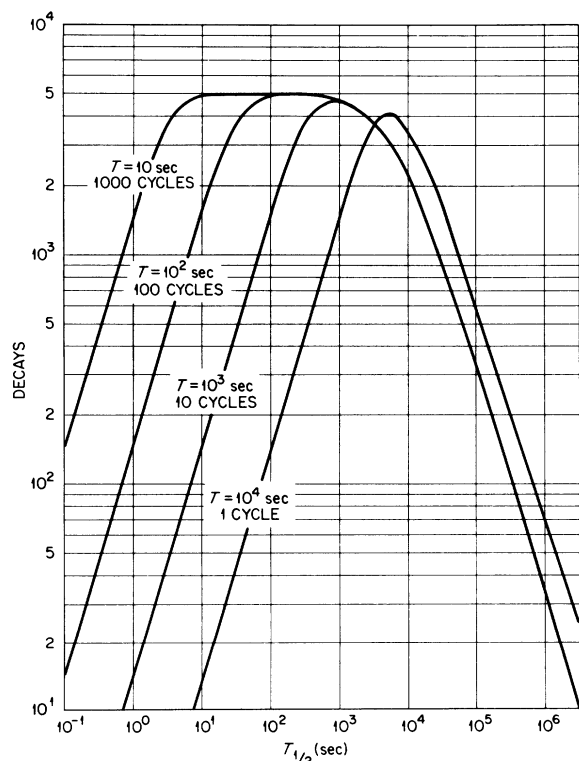


FIG. 2. Decays emanating from radioactivities during the detection periods for the production rate of one nucleus/sec. These are given as a function of the half-lives of the activities for the four bombarding conditions shown in the figure. In each cycle the target is bombarded for time T and then detection takes place for time T .

the four curves. The number of cycles is adjusted to give a total time of 2×10^4 sec. For example, 1000 cycles of 10-sec-irradiation-10-sec-detection period give maximum decays for activities with $T_{1/2} = 10 - 10^3$ sec. However, because the detection time should also be appropriate to obtain half-lives, this cycle time would only be suitable for $T_{1/2}$ up to about 40 sec. The decrease of all curves in Fig. 2 for $T_{1/2}$'s above 10^4 sec reflects the limited irradiation time and demonstrates the loss in sensitivity as half-lives of the products become increasingly longer.

γ -ray spectra were also taken with the target in beam with a Ge(Li) detector. In order that a correction could be applied for the angular distribution of the γ rays, the spectra were observed at both 90 and 30° relative to the incident beam.

III. RESULTS

Figure 3 gives an example spectrum of γ rays from the radioactive products. Above each peak is its energy, the nucleus to which the γ ray is attributed, and x , the number of nucleons emitted from the $^{16}\text{O} + ^{58}\text{Ni}$ system to give a nucleus of this mass. The details of identification as based on γ -ray energies and intensities and on half-lives of the radioactivities are contained in Appendixes A and B.

Representative examples of γ -ray yields as a function of time after an irradiation chosen to illustrate special points are given in Figs. 4-6. The example of the 635-keV γ ray in Fig. 4 demonstrates how a yield curve of a single γ ray can be used to ascertain the ratio of cross sections from two reactions resulting in two isobars, although in the particular case cited only a limit was obtainable. These yields are of γ rays emanating from the ^{60}Ni target after a 0.72-h-irradiation with 42-MeV ^{16}O ions. From its decay curve and energy, the 635-keV γ ray was identified as one from the first 2^+ state in ^{74}Se . The radioactive nucleus ^{74}Br , whose decay to ^{74}Se gives rise to the 635-keV γ ray, can be produced in two ways: (1) by direct creation through the $^{60}\text{Ni}(^{16}\text{O}, pn)$ reaction and (2) by radioactive decay of 16-min ^{74}Kr which is produced by the $^{60}\text{Ni}(^{16}\text{O}, 2n)$ reaction. The predicted decay curve for different ratios of the relative cross sections of the $(^{16}\text{O}, pn)$ and $(^{16}\text{O}, 2n)$ reactions were calculated and those for the ratios 2, 5, and 10 are plotted in Fig. 4. Comparison of these with the experimental points indicates the $(^{16}\text{O}, pn)$ reaction is greater than eight times the $(^{16}\text{O}, 2n)$ reaction for $E_{^{16}\text{O}} = 42$ MeV.

Another way in which the yield curves assisted in a few situations was to establish γ -ray doublets

and provide the relative intensities of the unresolved γ rays. The best example was for the 1039-keV γ ray from the ^{58}Ni target; its relative yield is given in Fig. 5. The energy was consistent with that of the strongest γ ray occurring in the decay chain of 44-min $^{70}\text{Se} \rightarrow 52\text{-min } ^{70}\text{As} \rightarrow ^{70}\text{Ge}$. But a calculated shape for a double decay with those half-lives and for our particular irradiation time did not agree with the experimental shape (see Fig. 5). However, there were other weaker transitions with energies $E = 744, 1114, 1708, \text{ and } 2019 \text{ keV}$, and relative intensities appropriate to the decay of ^{70}As whose yield curves did agree with this calculated shape. This is demonstrated in Fig. 6; the yields of the four γ rays were summed to improve the statistics. Thus, the 1039-keV peak is considered to be a doublet. A second member could be the strongest transition

in the decay of ^{66}Ga which would be produced by the $^{58}\text{Ni}(^{16}\text{O}, 2\alpha)^{66}\text{Ge}$ reaction followed by the chain decay of 2.4-h $^{66}\text{Ge} \rightarrow 9.4\text{-h } ^{66}\text{Ga} \rightarrow ^{66}\text{Zn}$. The shape of the calculated yield for this decay chain is shown in Fig. 5. By appropriate choice of amplitudes, the sum of the yield curves for the two 1039-keV γ rays fits the experimental points.

The method of obtaining cross sections from the radioactivities is briefly: The absolute yield of one γ ray associated with a particular product (the γ ray is listed in column 4 of Tables I and II) is used to determine the number of radioactive nuclei. Errors in this step include the uncertainties in the half-lives for the radioactivities, in the area in the full-energy γ -ray peak, in the efficiency of the Ge detector, and in the relative decay f (given in column 6 of Tables I and II) of the radioactivity through the γ ray under con-

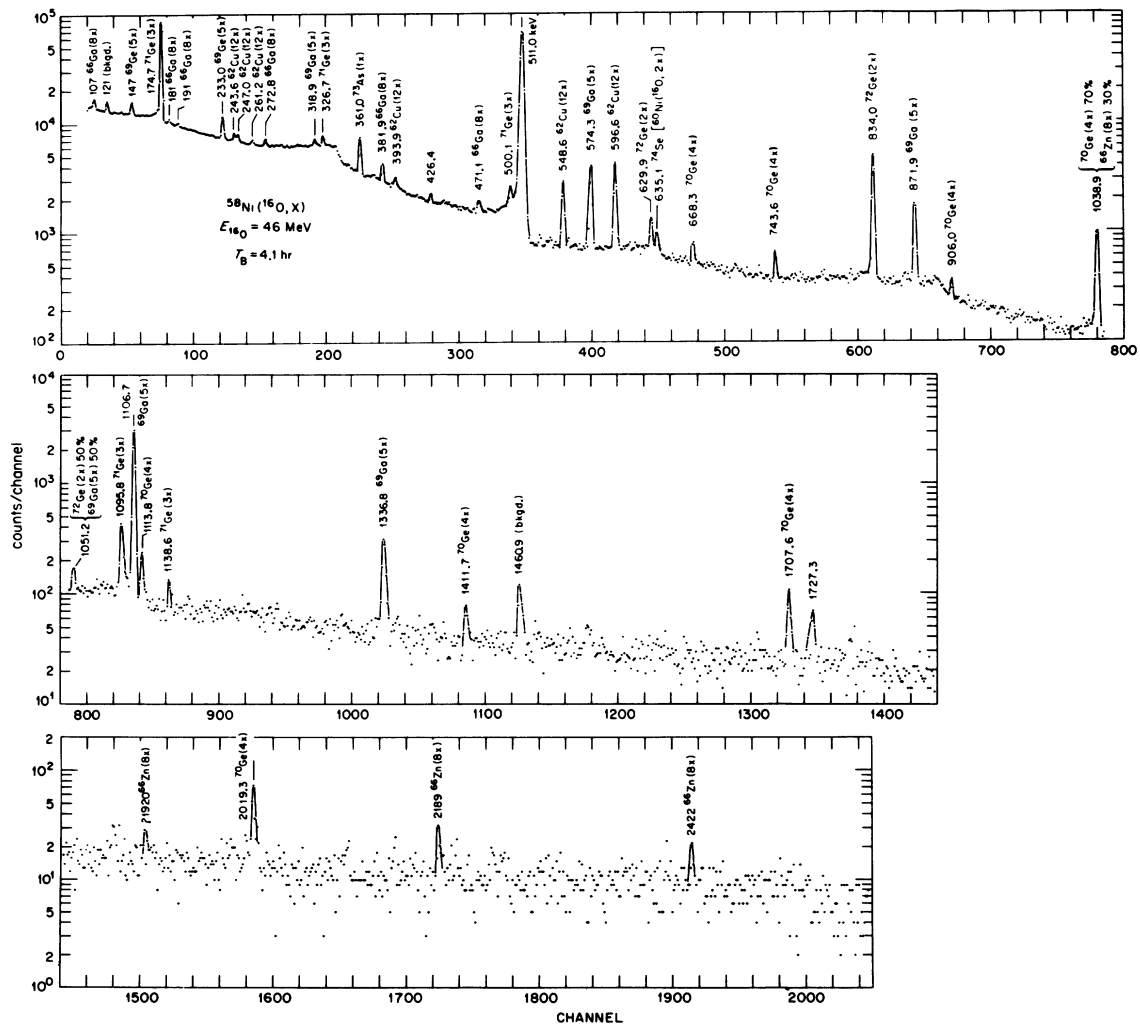


FIG. 3. Spectrum of γ rays from ^{58}Ni taken after a 4.1-h irradiation with 46-MeV ^{16}O ions.

sideration. (This included, for the low-energy γ rays, a correction for internal electron conversion.) The absolute efficiency of the Ge(Li) detector for a given geometry was determined typically to $\pm 6\%$ by means of a calibrated ^{226}Ra source. The quantity f in column 6 which comes from references cited in Appendixes A and B often did not have an error assignment. In these cases an assumed value, as shown in parentheses in column 6, is taken in calculating the errors in the cross sections. Even worse, f is not known in every instance.

The cross sections were then extracted from the number of radionuclides by appropriately accounting for the time of irradiation and detection, and for target thickness. The effect of the variation in beam current during the irradiations was included. The target thickness was determined from weight and area measurements with a combined uncertainty of $\pm 4\%$. Also because there was only one ^{58}Ni and one ^{60}Ni target, corrections for earlier irradiations were applied. This effect was minimized by doing the irradiations at the lower projectile energies first and generally separating irradiations of the same target by about a day.

For the in-beam γ ray study the cross sections were obtained from the $2 \rightarrow 0$ γ -ray intensity in even-mass cases assuming instantaneous decay, i.e., no isomeric levels. A correction was applied where necessary for additional population of the 2^+ state by radioactive decay, e.g., the decay of ^{72}Br to the 2^+ state in ^{72}Se . For the in-beam work the record of beam intensity is simple; only the integrated-beam current during the detection

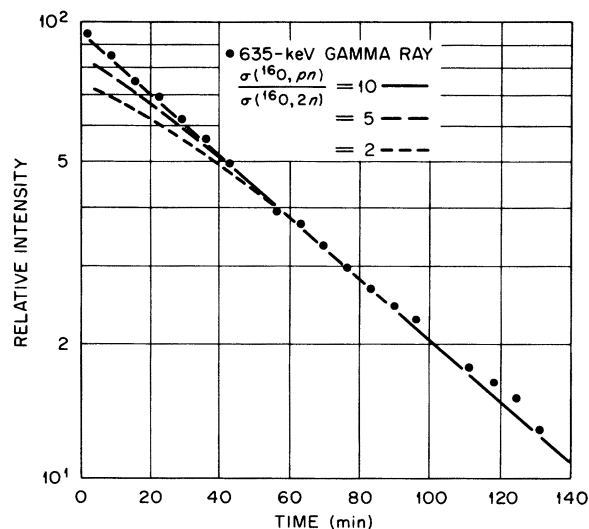


FIG. 4. Decay curves of the 635-keV γ ray from the ^{60}Ni target following a 0.72-h bombardment with 42-MeV ^{16}O ions.

period must be known.

The cross sections are summarized in the last three columns of Tables I and II. These have not been corrected for the fact that the target was thick (~ 5 MeV thick for the ^{16}O projectiles). Note that frequently we cannot establish which of several reactions causes a particular radioactivity; these possible reactions are then bracketed in column 2. Tables I and II also include upper limits on several reactions for a projectile energy of 46 MeV as based on upper limits for the intensities of the γ rays listed in column 4.

Curves were visually fitted to the thick-target cross-section results in Tables I and II, and from these curves the cross sections, corrected for the target thickness, were extracted. These cross sections, which were the principal goal of this work, are plotted in Figs. 7 and 8. Because there was only one measurement for the $^{58,60}\text{Ni}$ (^{16}O , ^{15}N) reactions, we show them in Figs. 7 and

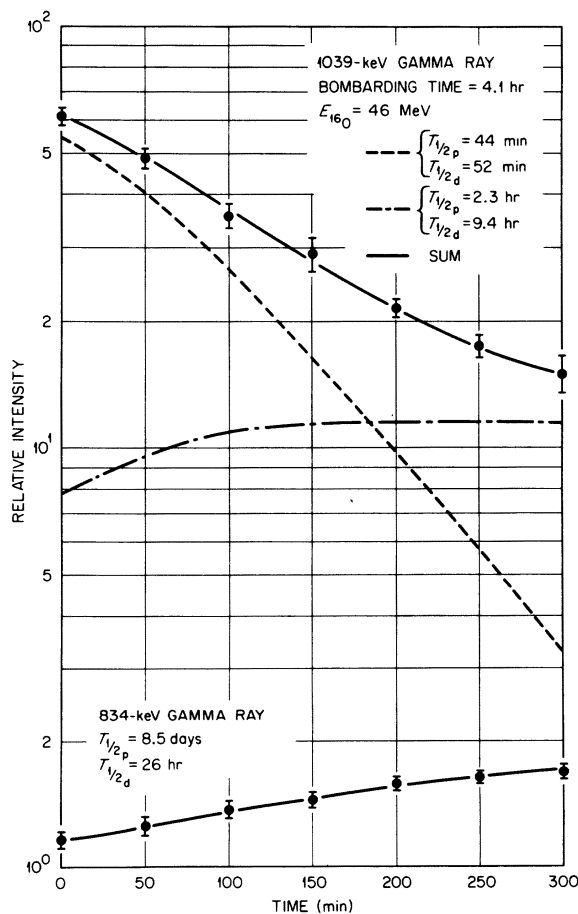


FIG. 5. Decay curves of the 1039- and 834-keV γ rays from the ^{58}Ni target following a 4.1-h bombardment with 46-MeV ^{16}O ions. The curves are calculated with the half-lives given in the figure.

8 at the average energy of the projectile in the target. In plotting the cross sections extracted from the in-beam studies, f was taken as 0.90 ± 0.10 . Although this value has not been measured, the strength of the $2 \rightarrow 0$ lines in the in-beam spectra suggests this is a conservative assumption.

An independent check of our results is obtained from a comparison to the recent work of Bair *et al.*⁸ They measured the total number of neutrons emitted in the $\text{Ni} + ^{16}\text{O}$ reactions as a function of projectile energy by means of a large graphite sphere with embedded BF_3 counters. A subset of their results for the ^{58}Ni target is illustrated in Fig. 9. The solid line gives the sum of the cross sections from our work for the major reactions in which neutrons are emitted [the

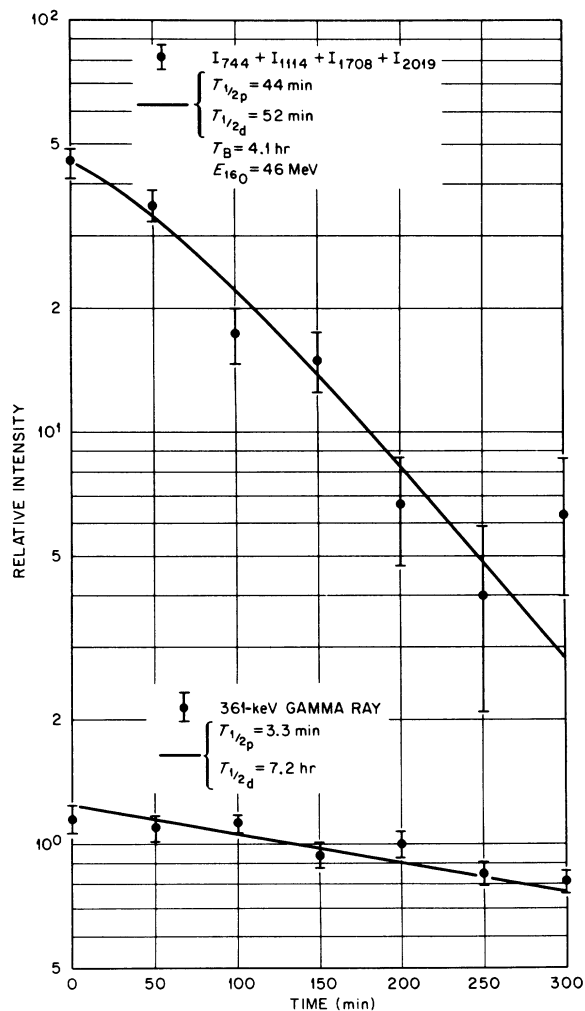


FIG. 6. Decay curves for the 361-keV γ ray and for the sum of the yields of the 744-, 1114-, 1708-, and 2019-keV γ rays from the ^{58}Ni target following a 4.1-h irradiation with 46-MeV ^{16}O ions. The curves are calculated with the half-lives given in the figure.

$(^{16}\text{O}, pn)$ and $(^{16}\text{O}, 2pn)$ reactions]. Although the cross sections for the $(^{16}\text{O}, \alpha n)$, $(^{16}\text{O}, p2n)$, and $(^{16}\text{O}, n)$ reactions were not uniquely determined, the results for the $^{60}\text{Ni} + ^{16}\text{O}$ case and the compound-nuclear calculations as discussed in Sec. IV, suggest they are small (a crude estimate gave $\sim 7\%$ of the total neutron cross section). That they are small is supported by the good agreement between the two measurements illustrated by Fig. 9.

IV. DISCUSSION

Several features are obvious from a casual observation of Figs. 7 and 8: All of the cross sections rise rapidly (this is because of the Coulomb barrier which occurs at 44 MeV for $r_0 = 1.45$ fm); the cross section is fragmented between a large number of exit channels; charged-particle emission strongly competes with neutron emission; and proton emission is larger for $^{58}\text{Ni} + ^{16}\text{O}$ than

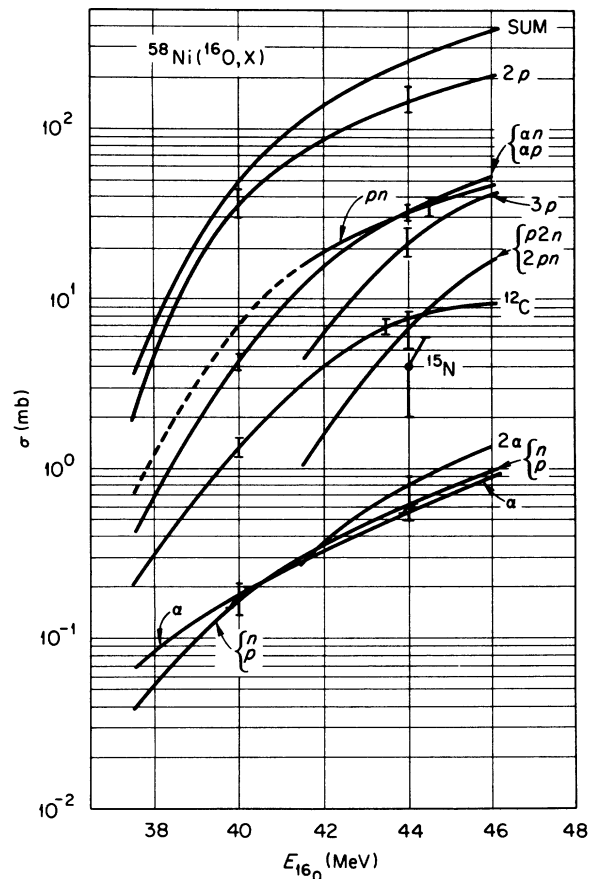


FIG. 7. Experimentally determined absolute cross sections for reaction products from ^{16}O ions incident on ^{58}Ni . Absolute errors are indicated by the flags. The energies are in the laboratory system. The dashed portion of the $(^{16}\text{O}, pn)$ cross section is deduced from Ref. 8.

$^{60}\text{Ni} + ^{16}\text{O}$ reactions. This last fact was already pointed out by Nolte *et al.*⁷ and is supported by a corresponding decrease in cross sections for total neutron emission as measured by Bair *et al.*⁸ (note Figs. 9 and 14). Both groups find this trend continuing for the heavier Ni isotopes. Qualitatively, the strong competition of charged-particle emission is explainable if the energy available to p and α emission is sufficiently greater than that available to neutron emission to compensate for the Coulomb barrier. This energy difference becomes greater with increasing neutron deficiency and thus the $^{58}\text{Ni} + ^{16}\text{O}$ interaction would be expected to produce more charged-particle emission than that for the $^{60}\text{Ni} + ^{16}\text{O}$ interaction.

We have compared the sum of the cross sections in Figs. 7 and 8 to the reaction cross section calculated with an optical model using the computer program GENOA developed by Perey,⁹ and the relative production of reaction products with that given for statistical decay of a compound nucleus.

Table III shows three sets of optical-model parameters appropriate to reactions between ^{16}O and Ni. The potential wells have a Woods-Saxon form and $R = r_0(A_T^{1/3} + A_P^{1/3})$. The parameters of Obst, McShan, and Davis¹⁰ were determined from the differential elastic scattering results of ^{16}O from ^{56}Fe taken every 2 MeV for $E_{\text{lab}} = 38\text{--}60$ MeV. After first fixing the geometrical factors $r_0 = r'_0$ and $a = a'$ at the best average values, they varied the real and imaginary well depths to give the best fit at each projectile energy. Set 1 from Christensen *et al.*¹¹ was deduced from a four-parameter fit ($V, W, r_0 = r'_0$, and $a = a'$) to the differential elastic cross section for scattering of 44-MeV ^{16}O ions from ^{58}Ni . Set 4 of Christensen *et al.* includes the additional flexibility in that r, r', a , and a' are independently varied; the six parameters were selected to yield best fits to the 44- and 60-MeV elastic differential cross sections. This latter set gave generally reasonable fits to elastic and inelastic scattering data for $E_{^{16}\text{O}} = 35\text{--}$

TABLE I. Products of the $^{58}\text{Ni}(^{16}\text{O}, X)Y$ reactions. The third, fourth, fifth, and sixth columns identify the technique used (A =activation, I =in beam), γ -ray transition used to obtain the cross section, the nucleus in which the transition occurs, and the ratio f of this γ -ray intensity to the total intensity, respectively. The last three columns are the cross sections uncorrected for target thickness.

X	Y	Method	E_γ (keV)	Nucleus	f	σ (mb)		
						$E_{^{16}\text{O}}$ (MeV)=38 ΔE (MeV) ^a = 4.1	42 4.0	46 3.8
n	^{73}Kr	A	361.0	(^{73}As)	0.97 (± 0.01)	0.020 \pm 0.005	0.19 \pm 0.03	0.65 \pm 0.07
p	^{73}Br							
2n	^{72}Kr	A	310	(^{72}Br)	0.21			<1.0
2n	^{72}Kr	A	862.0	(^{72}Se)	0.73 \pm 0.01		7.8 \pm 0.7	32 \pm 3
pn	^{72}Br							
2p	^{72}Se	A	834.0	(^{72}Ge)	0.77 (± 0.07)	0.62 \pm 0.50	39 \pm 8	147 \pm 31
2p	^{72}Se	I	862.0	(^{72}Se)			38 \pm 3/f	141 \pm 11/f
p2n	^{71}Br	A	147	(^{71}As)	0.48 (± 0.04)		0.4 \pm 0.2	8 \pm 2
2pn	^{71}Se							
3p	^{71}As	A	174.7	(^{71}Ge)	0.82 \pm 0.02	<0.06	1.7 \pm 0.2	24 \pm 4
α	^{70}Se	A	1038.9	(^{70}Ge)	0.82 \pm 0.01	0.05 \pm 0.03	0.19 \pm 0.03	0.60 \pm 0.05
αn	^{69}Se	A	{ 233.0 1106.7	(^{69}Ge) (^{69}Ga)	0.10 \pm 0.02 0.26 (± 0.05)	0.14 \pm 0.08	6.6 \pm 1.1 4.6 \pm 1.1	37 \pm 7 33 \pm 7
αp	^{69}As							
$\alpha 2n$	^{68}Se	A	980	(^{68}As)				<0.07/f
αpn	^{68}As		1075	(^{68}Ge)				<0.1/f
2 α	^{66}Ge	A	{ 381.9 1038.9	(^{66}Ga) (^{66}Zn)	0.29 \pm 0.03 0.38 (± 0.05)	0.04 \pm 0.04	0.14 \pm 0.03 0.27 \pm 0.13	0.87 \pm 0.14 0.87 \pm 0.27
2 αn	^{65}Ge							
2 αp	^{65}Ga	A	752	(^{65}Zn)	0.08			<9
^{12}C	^{62}Zn	A	596.6	(^{62}Cu)	0.227 \pm 0.004	0.10 \pm 0.03	1.6 \pm 0.2	7.7 \pm 0.7
^{14}C	^{60}Zn	A	1332.5	(^{60}Ni)	0.87			<0.5
^{14}N	^{60}Cu							
^{14}O	^{60}Ni	I	1332.5	(^{60}Ni)				<3/f
^{15}N	^{59}Cu	A	1302	(^{59}Ni)	0.10 (± 0.03)		<0.9	4 \pm 2
^{15}O	^{59}Ni	I	878	(^{59}Ni)				<5/f
^{17}O	^{57}Ni	A	1377.6	(^{57}Co)	0.79			<0.6

^a Energy loss in target.

TABLE II. Products of the $^{60}\text{Ni}(^{16}\text{O}, X)Y$ reactions.

X	Y	Method	E_Y (keV)	Nucleus	f	$E_{^{16}\text{O}}$ (MeV) = 38 ΔE (MeV) ^a = 6.8	σ (mb)	
							42 6.6	46 6.3
n	^{75}Kr	A	133	(^{75}Br)				0.2/f
n	^{75}Kr	A	286.8	(Se)	0.93 ± 0.02	0.040 ± 0.006	0.65 ± 0.06	1.58 ± 0.16
p	^{75}Br							
2n	^{74}Kr	I	429	(^{74}Kr)			1.2 ± 0.1/f	8.9 ± 0.6/f
pn	^{74}Br	A	634.8	(^{74}Se)	0.87 ± 0.11	0.69 ± 0.09	30 ± 4	95 ± 12
2p	^{74}Se	I	634.8	(^{74}Se)		0.6 ± 0.2/f	18 ± 6/f	73 ± 23/f
p2n	^{73}Br	A	700	(^{73}Se)	0.13			<1.5
2pn	^{73}Se (7.2 h)	A	361.0	(^{73}As)	0.97(± 0.01)	0.005 ± 0.005	1.34 ± 0.12	16 ± 2
	^{73}Se (42 min)	A	394	(^{73}As)	0.07			<1.2
α	^{72}Se	I	862	(^{72}Se)				<5/f
αn	^{71}Se	A	147	(^{71}As)	0.48(± 0.04)		1.06 ± 0.21	4.9 ± 0.9
αp	^{71}As	A	174.7	(^{71}Ge)	0.82(± 0.02)	0.20 ± 0.03	6.1 ± 0.8	30 ± 3
$\alpha 2n$	^{70}Se	A	1039	(Ge)	0.82			<0.5
αpn	^{70}As							
$\alpha 2p$	^{70}Ge	I	1039	(^{70}Ge)				<1.0/f
2 αn	^{67}Ge	A	167	(^{67}Ga)	1.14			<0.13
2 αp	^{67}Ga	A	185	(^{67}Zn)	0.21			<2.8
^{12}C	^{64}Zn	I	992	(^{64}Zn)				<4/f
^{14}C	^{62}Zn	A	597	(^{62}Cu)	0.20			<1.0
^{14}O	^{62}Ni	I	1172	(^{62}Ni)				<2/f
^{15}N	^{61}Cu	A	656.2	(^{61}Ni)	0.10(± 0.02)		<0.6	1.9 ± 0.5
^{15}O	^{61}Ni	I	909	(^{61}Ni)				<1/f
^{17}O	^{59}Ni	I	878	(^{59}Ni)				<0.6/f
^{17}F	^{59}Co	I	1099	(^{59}Co)				<0.6/f

^a Energy loss in target.

60 MeV.

Comparison of the sum of the reaction cross sections given in Figs. 7 and 8 to the total reaction cross sections calculated with the three sets of optical-model parameters, is illustrated in Fig. 10. Since it is possible some weak exit channels went undetected, the ratio $\sigma_{\text{exp}}/\sigma_{\text{cal}}$ should be ≤ 1.0 . Also the cross section for the inelastic nuclear scattering and Coulomb excitation were not included. Indeed, inclusion of the Coulomb excitation cross section does worsen the agreement with the calculated cross sections at low projectile energies where its cross section predominates over that of other reactions. For example, for 38-MeV ^{16}O ions on ^{60}Ni , where the Coulomb ex-

citation cross section for the first 2^+ state is 53 mb, as compared to 16 mb for the sum of the reactions shown in Fig. 8, the ratio $\sigma_{\text{exp}}/\sigma_{\text{cal}}$ calculated for the three sets of optical-model parameters contained in Table III is, respectively, 2.8, 5.2, and 9.9. This suggests that the shape of the elastic differential cross sections from which the optical-model parameters are deduced, is less sensitive to the long-range Coulomb interaction than to the short-range nuclear interaction.

Le Beyec and collaborators^{12, 13} have used the onset of nuclear reactions to determine the minimum distance of approach assuming a classical Coulomb radius and found for ^{40}Ar on ^{164}Dy , an $r_{\text{Coul}} = 1.45$ fm, whereas for ^{84}Kr on ^{72}Ge and ^{116}Cd ,

TABLE III. Optical-model parameters used for ^{16}O projectiles on Ni targets.

Reference	V (MeV)	r_0 (fm)	a (fm)	W (MeV)	r'_0 (fm)	a' (fm)	r_{Coul} (fm)
Obst <i>et al.</i> (Ref. 10)	19.8 + 0.16E	1.25	0.6	0.5–11.7 ^a	1.25	0.6	1.35
Christensen <i>et al.</i> (Ref. 11)							
Set 1	29.43	1.30	0.491	2.43	1.30	0.491	1.25
Set 4	22.05 + (E – 40)0.16	1.30	0.533	1.59 + (E – 40)0.19	1.37	0.375	1.25

^a Values of W at $E_{\text{lab}} = 36, 38, 40, 42, 44,$ and 46 MeV are, respectively, $\approx 0.5, 5.0, 9.4, 11.7, 11.7,$ and 11.3 MeV.

$r_{\text{Coul}} = 1.32$ fm. The energy threshold of ~ 36 MeV for ^{16}O on $^{58,60}\text{Ni}$ obtained in this work and from the measurements of Bair *et al.*⁸ corresponds to the much larger distance of $r_{\text{Coul}} = 1.78$ fm.

To calculate the relative population of the reaction products assuming statistical decay of a compound nucleus, we used a computer program developed by Blann.³ Briefly, it considers the statistical probability for decay of the compound system and for decay from each resulting nucleus by proton, neutron, and α -particle emission until a level is reached in a nucleus which is stable to particle emission. The probability for decay of a particle of energy ϵ was taken as the product of the transmission coefficients $T_{ij}(\epsilon)$ times an appropriate statistical factor summed over all momenta, and of the level density whose dependence on excitation energy E is

$$\rho(E) \propto \frac{1}{(E - \delta)^2} e^{2[\alpha(E - \delta)]^{1/2}}. \quad (1)$$

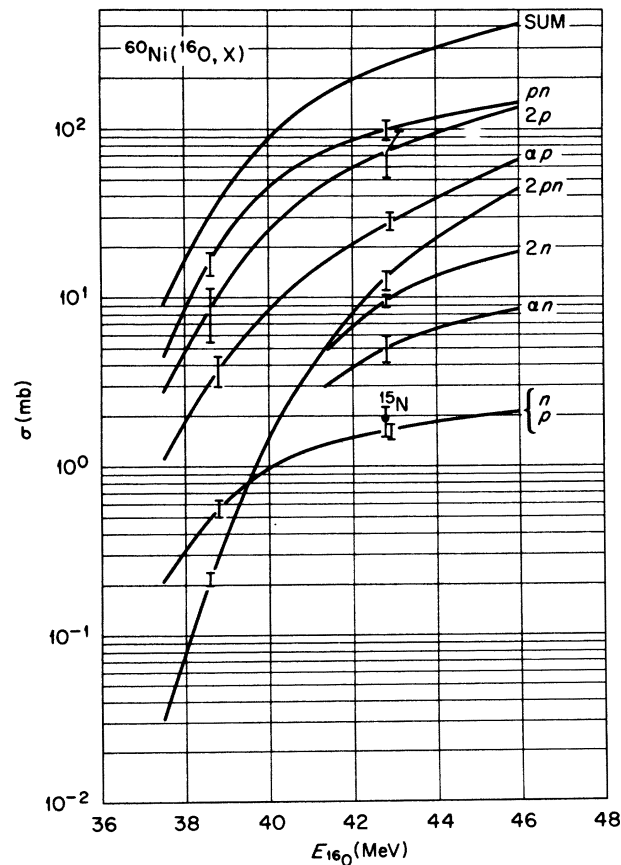


FIG. 8. Experimentally determined absolute cross sections for reaction products from ^{16}O ions incident on ^{60}Ni . Absolute errors are indicated by the flags. The energies are in the laboratory system.

The quantity \mathcal{Q} is the level-spacing parameter, and δ the pairing parameter is an adjustment to account for the difference in level density between odd-odd, even-odd, and even-even nuclei. In our calculations $\delta = 0, \Delta$, and 2Δ , respectively, for these three classes of nuclei. Blann's program was modified so that the transmission coefficient were calculated with a subroutine adapted from work of Smith.¹⁴ The optical-model parameters for the neutron, proton, and α -particle emission are, respectively, those given in Refs. 15-17. To reduce computer time and storage-space requirements, the excitation energies of each nucleus were considered in 1-MeV "bins." γ -ray emission was assumed not to compete with neutron emission nor with emission of charged particles if their inverse-reaction cross section was greater than 1 mb; conversely, below this 1-mb cross section, charged-particle emission did not compete with γ -ray emission. For the particular case of the $^{16}\text{O} + \text{Ni}$ system, this assumption caused the charged-particle decay probability to be set equal to 0 for $E_p \leq 2$ MeV and $E_\alpha \leq 6$ MeV.

For the calculated curves shown in Figs. 11 and 12, values of Δ and \mathcal{Q} were, respectively, 1.4 MeV and $A_{\text{CN}}/8 \text{ MeV}^{-1}$. Binding energies came from the mass excesses compiled by Wapstra and Gove.¹⁸ Cases not listed were obtained from extrapolation of β disintegration energies. The unknown \mathcal{Q} values for the $^{16}\text{O} + ^{58,60}\text{Ni}$ reactions were taken to be, respectively, -2.86 and -0.060 MeV as given

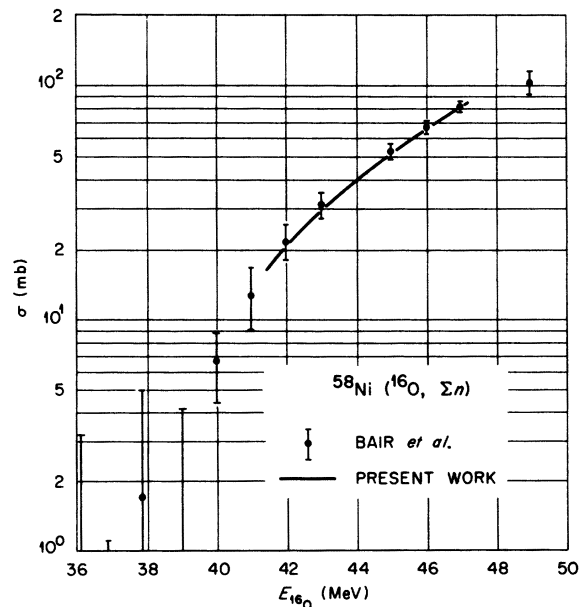


FIG. 9. Comparison of the cross sections for neutron emission obtained by Bair *et al.*, (Ref. 8) and in the present work for ^{16}O irradiation of ^{58}Ni . The uncertainty in our curve is $\pm 9\%$.

in Ref. 19.

Probably the most significant limitation of the version of Blann's program³ used in the present calculations is that the spin of the levels is not included. This is equivalent to assuming the same level density as given by Eq. (1) for all spins. This restriction will cause qualitatively several differences in the predicted yield curves: (1) They will rise and fall more rapidly with projectile energy, (2) they will peak at a lower projectile energy, and (3) their peak cross sections will be larger.²⁰

The predictions as illustrated in Figs. 11(b) and 12(b) for the different channels are given as a percent of the total decay. The experimental results are plotted in a similar manner in Figs. 11(a)

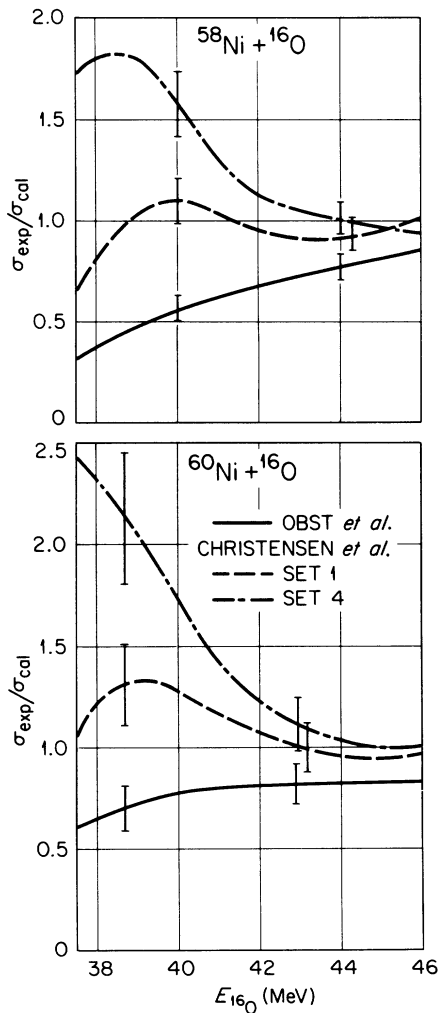


FIG. 10. Comparison of the sum of the experimental cross sections shown in Figs. 7 and 8 with those calculated with the three sets of optical-model parameters listed in Table III. The errors reflect the uncertainty in the measured cross sections.

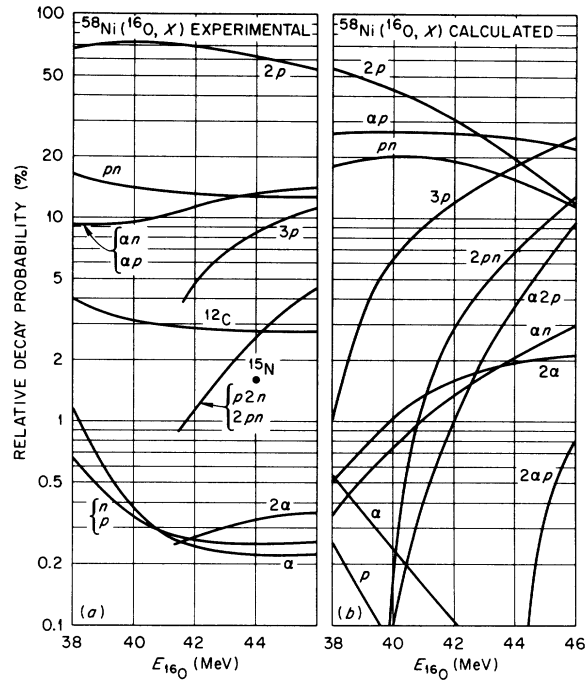


FIG. 11. Comparison of the relative experimental cross sections for the $^{58}\text{Ni}(^{16}\text{O}, X)$ reactions with those calculated for the statistical decay of a compound nucleus.

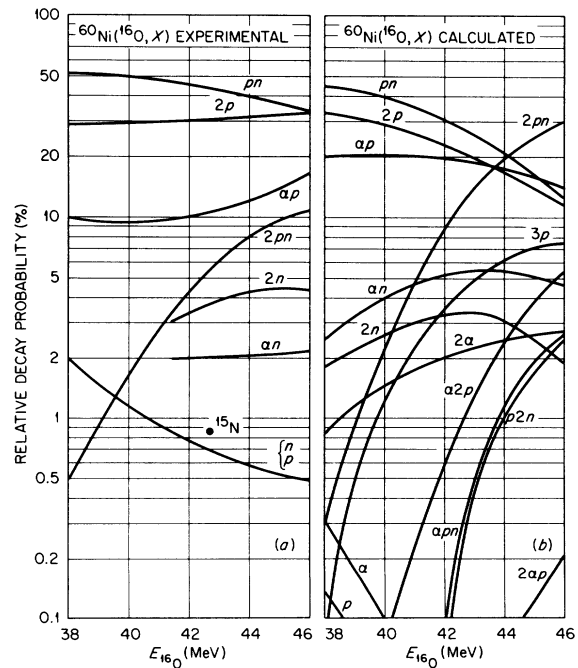


FIG. 12. Comparison of the relative experimental cross sections for the $^{60}\text{Ni}(^{16}\text{O}, X)$ reactions with those calculated for the statistical decay of a compound nucleus.

and 12(a). A comparison of these figures shows that the general features but not the details of the experimental data are given by the theory. Predictions that the $(^{16}\text{O}, 2p)$, $(^{16}\text{O}, pn)$, and $(^{16}\text{O}, \alpha p)$ cross sections are the largest at the lower projectile energies are consistent with the experimental results. But the experimental values for the one-nucleon emission are significantly larger than that given by the calculations and the experimental three-nucleon cross sections are smaller than predicted. These differences are attributable at least in part to the assumption that the level density is independent of spin.

Although extensive efforts were not made to improve agreement by varying the input parameters, we do show by means of Fig. 13 the sensitivity of the relative cross sections for the two-particle emitting channels from the $^{16}\text{O} + ^{60}\text{Ni}$ system to changes in several of the parameters. It includes three examples in which a different value was taken for a nuclear mass whose value was

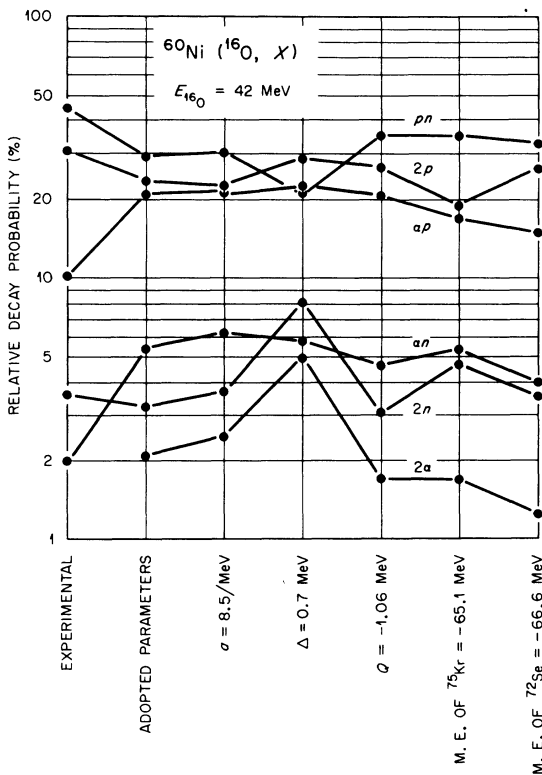


FIG. 13. Dependence of predicted cross sections for $^{60}\text{Ni}(^{16}\text{O}, X)$ reactions at $E_{^{16}\text{O}} = 42$ MeV on various input parameters. Only the parameter noted in the figure is changed from the "adopted-value" set. The adopted values for those parameters were: $\bar{G} = 7.5$ MeV $^{-1}$, $\Delta = 1.4$ MeV, Q for the $^{16}\text{O} + ^{60}\text{Ni}$ system = -0.060 MeV, mass excess of $^{75}\text{Kr} = -64.1$ MeV, and mass excess of $^{72}\text{Se} = -67.6$ MeV.

based only on systematics. For the most part changes in cross section are moderate although a reduction of the pairing energy by 0.7 MeV did increase the $(^{16}\text{O}, 2n)$ and $(^{16}\text{O}, 2\alpha)$ cross sections by a factor of 2. Note that none of the parametric changes tried give cross sections for the αp and αn channels as small as measured or as large as the experimental pn channel.

The reaction listed as $(^{16}\text{O}, ^{12}\text{C})$ for the ^{58}Ni reaction would give the same product as 3α emission. However, the predicted relative $^{58}\text{Ni}(^{16}\text{O}, 3\alpha)$ cross section is $<0.01\%$. Presumably the $(^{16}\text{O}, ^{12}\text{C})$ reaction as well as the $(^{16}\text{O}, ^{15}\text{N})$ reaction is direct.

In several cases, our experimental results cannot decide between one of several reactions. If we take the theoretical predictions as being reasonably close to the physical situation, then cross sections for $p2n-2pn$ and $\alpha p-\alpha n$ channels due to the $^{16}\text{O} + ^{58}\text{Ni}$ interaction [see Fig. 11(a)] are predominantly due to $2pn$ and αp emission. For both ^{58}Ni and ^{60}Ni , the calculations favor the $(^{16}\text{O}, p)$ reaction over the $(^{16}\text{O}, n)$ reaction.

The reaction consistent with the available energy that would produce the nucleus farthest from stability in this study is $^{58}\text{Ni}(^{16}\text{O}, 2n)$. The calculated $^{58}\text{Ni}(^{16}\text{O}, 2n)$ decay is $\sim 0.025\%$ of the total decay for $E_{^{16}\text{O}} = 46$ MeV or ~ 0.1 mb. We could only establish experimentally the limit of <1 mb at $E_{^{16}\text{O}} \approx 44$ MeV.

V. SUMMARY

We found that for reactions induced by bombarding $^{58,60}\text{Ni}$ with 38- to 46-MeV ^{16}O ions, charged-particle emission strongly competes with neutron emission thereby reducing appreciably the cross section for producing nuclei far from stability. The general features of the relative excitation of the exit channels is accounted for by predictions based on the statistical decay of a compound nucleus except for the two channels $(^{16}\text{O}, ^{12}\text{C})$ and $(^{16}\text{O}, ^{15}\text{N})$ which are probably due to direct reactions. Some differences between the calculated and measured cross sections, namely the long tail of the experimental cross sections in which one nucleon is emitted, and the smaller experimental cross sections for the three nucleon channels, could be due to the assumption in the calculations that the level density is independent of spin. However, it is doubtful that other differences, such as the calculated $(^{16}\text{O}, \alpha n)$, $(^{16}\text{O}, \alpha p)$, and $(^{16}\text{O}, 2\alpha)$ cross sections being larger than measured, are caused by this approximation. Some possible causes may be γ -ray competition, variability of level density from one nucleus to another, incorrect binding energies, and noncompound-nuclear processes.

The sum of the measured cross sections agree to within $\sim 20\%$ of the reaction cross section for $E_{^{16}\text{O}} = 44\text{--}46$ MeV as calculated with three different sets of optical-model parameters^{10,11} (see Fig. 10). At lower energies, down to 37.5 MeV, the variation in agreement between the experimental results and the three calculated values suggests that the total reaction cross section can help in the selection of the correct optical-model parameters.

ACKNOWLEDGMENTS

We wish to express our appreciation to Dr. Marshall Blann for his program and his guidance in its use and modification. Also we express our thanks to the support personnel, Jim Johnson, George Wells, Frank Dicarlo, Dick Cumby, and Dave Galbraith, who assisted in various ways. We are deeply indebted to W. T. Milner for his development of several excellent data-reduction computer programs.

APPENDIX A. $^{58}\text{Ni}(^{16}\text{O}, X)$ REACTIONS

In this and the following Appendix we discuss the evidence for the different reaction products. Since our principal objective is to establish which nuclei are produced and not to survey all of the studies of a given radioactivity, we have generally compared our γ -ray results to only one of the previous works. The degree of confidence for identifying a particular product depends on the extent of similarity between the γ -ray energies and intensities, and half-life for decay determined here, and those previously reported. (Refer to column 2 in Tables I and II for the reaction products discussed in this and the following Appendix.) The quantity x refers to either protons or neutrons. Three of the delayed γ rays resulting from the irradiated ^{58}Ni target were not identified; their energies in keV (and half-lives) are 426.4 ($0.9 \pm_{-0.4}^{+1.5}$ h), 977.2 (0.5 ± 0.3 min), and 1727.3 (> 5 h).

A. $^{58}\text{Ni}(^{16}\text{O}, x)$ reactions

The presence of these reactions was based on the observation of a 361.0 ± 0.5 -keV γ ray which has an energy like that of the predominant transition in the decay of 7.2-h $^{73}\text{Se}^{21,22}$; its yield as a function of time is in acceptable agreement with the decay of 3.3-min $^{73}\text{Br} \rightarrow 7.2\text{-h } ^{73}\text{Se} \rightarrow ^{73}\text{As}$ (see Fig. 6). We searched for the known γ rays from the decay of ^{73}Br and within large errors found possible 700- and 931-keV γ rays which are two of the strongest transitions in its decay²³; their yield gives a cross section of 1.0 ± 1.0 mb for $E_{^{16}\text{O}} = 46$ MeV which is consistent with the value

of 0.65 ± 0.07 mb deduced from the 361-keV transition.

To determine the division of cross section between the $^{58}\text{Ni}(^{16}\text{O}, n)^{73}\text{Kr}$ and $(^{16}\text{O}, p)^{73}\text{Br}$ reactions requires detection of γ rays from the decay of ^{73}Kr . This 25.9-sec activity was only recently studied in any detail by Davids and Goosman.²⁴ We did not observe any of the γ rays and at best, from the strongest γ ray with $E = 178.1$ keV, could only place a limit (2.5 mb for 46-MeV ^{16}O projectiles) that is significantly larger than obtained for the cross sections of the $(^{16}\text{O}, n)$ and $(^{16}\text{O}, p)$ reactions together.

B. $^{58}\text{Ni}(^{16}\text{O}, 2x)$ reactions

The sum of ^{72}Br and ^{72}Kr production was established on γ rays attributed to the decay of ^{72}Br . Besides the 454.7-, 774.7-, 862.0-, and 1316.7-keV γ rays which energetically fit between levels assigned to ^{72}Se by Nolte *et al.*,⁷ more than 25 others with appropriate half-lives for ^{72}Br were observed. The construction of a decay scheme for ^{72}Se deduced from singles and coincident γ -ray spectra is discussed in a separate paper.⁵ Recently, Davids and Goosman^{24,25} and Schmeing *et al.*²⁶ produced ^{72}Kr by irradiating ^{58}Ni with ~ 53 -MeV ^{16}O ions. The strongest γ rays in their experiments ($E = 310$ and 415 keV) were not observed in our spectra and led to an upper limit of 1.0 mb for the $^{58}\text{Ni}(^{16}\text{O}, 2n)$ reaction for $E_{^{16}\text{O}} = 46$ MeV.

Three of the strongest γ rays in ^{72}Ge resulting from the decay chain 8.5-day $^{72}\text{Se} \rightarrow 26\text{-h } ^{72}\text{As} \rightarrow ^{72}\text{Ge}$ were observed. Their energies of 629.9 ± 0.5 , 834.0 ± 0.5 , and 1051.2 ± 0.8 keV and relative intensities, 11 ± 1 , 100, and 0.8 ± 0.3 , are consistent with those reported by Camp.²⁷ (The intensity of the 1051-keV γ ray had to first be corrected for that of a γ ray of the same energy in ^{69}Ga .) Also the 834-keV γ ray yield as a function of time is compatible with the double decay as exemplified in Fig. 5. Production of ^{72}Se is by the $^{58}\text{Ni}(^{16}\text{O}, 2p)$ reaction and by decay of ^{72}Br . Since we have already determined ^{72}Br production we can deduce the $(^{16}\text{O}, 2p)$ cross section. Still another estimate of the $(^{16}\text{O}, 2p)$ cross section was obtained from the ^{72}Se γ rays in the in-beam spectra.^{7,28}

C. $^{58}\text{Ni}(^{16}\text{O}, 3x)$ reactions

Because a literature search revealed no information about the decays of ^{71}Kr and ^{71}Br , their possible production via the $^{58}\text{Ni}(^{16}\text{O}, 3n)$ and $(^{16}\text{O}, p2n)$ could not be ascertained. Probably the $^{58}\text{Ni}(^{16}\text{O}, 3n)$ reaction is energetically impossible until $E_{^{16}\text{O}} \approx 50$ MeV.

The radioactivity ^{71}Se (Ref. 29) was identified

principally by the 147-keV γ ray. This line was actually found to be a composite of a 5-min component attributed to the decay of ^{71}Se and a 16-min component ascribed to the decay of ^{69}As . Other γ rays with energies, intensities, and half-lives supporting this ^{71}Se assignment were observed at 977 ± 2 , 1095.1 ± 0.6 , 1242.3 ± 1.0 , and 1269.4 ± 1.0 keV.

γ rays with energies of 174.7 ± 0.8 , 362.7 ± 0.7 , 500.1 ± 0.6 , 921 ± 1 , 1095.8 ± 0.6 , 1138.6 ± 0.8 , and 1213 ± 1 keV and with relative intensities compatible with those reported by Murray, Sanderson, and Willmott³⁰ for the decay of ^{71}As to ^{71}Ge were identified. After correcting for the decay of ^{71}Se to ^{71}As , the remaining ^{71}As yield gives the $^{58}\text{Ni}(^{16}\text{O}, 3p)$ cross section.

D. $^{58}\text{Ni}(^{16}\text{O}, \alpha)$ reaction

Production of ^{70}As was established by nine γ rays of appropriate energy and relative intensity³¹ ($E_\gamma = 668.3 \pm 0.6$, 743.6 ± 0.6 , 906.0 ± 0.7 , 1038.9 ± 0.7 , 1113.8 ± 0.6 , 1411.7 ± 0.7 , 1522 ± 1 , 1707.6 ± 0.6 , and 2019.3 ± 0.7 keV). Their yields are consistent with the double decay of 44-min ^{70}Se - 52-min ^{70}As - ^{70}Ge (see the example given in Fig. 6), where ^{70}Se would be produced in the $^{58}\text{Ni}(^{16}\text{O}, \alpha)$ reaction.

E. $^{58}\text{Ni}(^{16}\text{O}, \alpha x)$ reactions

Strong evidence for production of the radioisotope ^{69}Ge was provided by γ rays observed at 318.9 ± 0.8 , 553 ± 1 , 574.3 ± 0.5 , 871.9 ± 0.5 , 1106.7 ± 0.5 , and 1336.8 ± 0.5 keV.³² There was also evidence for its precursor ^{69}As (Ref. 33) as based on γ rays with energies of 147 ± 1 , 233.0 ± 0.7 , 287.4 ± 0.8 , 374.1 ± 0.8 , and 398.5 ± 0.8 keV. The half-life for ^{69}As deduced from their yield curve is 16 ± 1 min. Because nothing is known about the decay of ^{69}Se , we could only determine the combined cross section for the $^{58}\text{Ni}(^{16}\text{O}, \alpha n)$ and $(^{16}\text{O}, \alpha p)$ reactions. (There is insufficient energy for these reactions to be due to emission of five nucleons for $E_{^{16}\text{O}} < 50$ MeV.) The cross sections were calculated from the γ rays both from the decay of ^{69}As and from ^{69}Ge .

F. $^{58}\text{Ni}(^{16}\text{O}, \alpha 2x)$ reactions

The only reference found on the γ rays from the decay of 3.2-h ^{68}Se and 5.7-min ^{68}As was that of Bilge and Boswell.³⁴ Although they only gave γ -ray energies as determined with a NaI detector, an illustration in their paper indicated one of the stronger ^{68}Ge γ rays had an energy of 1075 keV; the only γ ray observed in ^{68}As was at 980 keV. Assuming the energies of the 980- and 1075-keV

γ rays are within 10 keV of the correct value, we obtained the limits for the $^{58}\text{Ni}(^{16}\text{O}, \alpha pn)$ and $(^{16}\text{O}, \alpha 2n)$ reactions given in Table I. Because of the very long half-life of ^{68}Ge , no significant limit could be put on the $^{58}\text{Ni}(^{16}\text{O}, \alpha 2p)$ cross section.

G. $^{58}\text{Ni}(^{16}\text{O}, 2\alpha)$ reaction

The residual nucleus ^{66}Ge (Ref. 35) in this reaction was clearly identified by γ rays at 181 ± 2 , 191 ± 2 , 272.8 ± 0.8 , 381.9 ± 0.5 , 471.1 ± 0.8 , and 537 ± 1 keV which decayed with an average half-life of 2.2 ± 0.3 min. Additional support was provided by (1038.9 ± 0.7) -, (1919.8 ± 1.5) -, (2188.9 ± 1.5) -, and (2421.7 ± 1.5) -keV γ rays attributable to the decay of ^{66}Ga to ^{66}Zn .³⁶ Cross sections deduced from the γ rays of both the decay of ^{66}Ga and ^{66}Ge are in agreement.

H. $^{58}\text{Ni}(^{16}\text{O}, 2\alpha x)$ reactions

A limit was placed on these reactions from the absence of γ rays from the decay of 15-min ^{65}Ga to ^{65}Zn .³⁷ The lowest value as given in Table I was based on the limit of a 752-keV γ -ray yield.

I. $^{58}\text{Ni}(^{16}\text{O}, ^{12}\text{C})$ reaction

γ rays which were observed at 243.6 ± 0.9 , 247.0 ± 0.9 , 261.2 ± 0.9 , 393.9 ± 0.7 , 548.6 ± 0.5 , and 596.6 ± 0.5 keV establish the presence of the residual product ^{62}Zn .³⁸ Although ^{62}Cu is also unstable 99.6% of its decays are to the ground state of ^{62}Ni (Ref. 39) and thus, not surprisingly, its γ rays were not seen.

J. One- and two-nucleon transfer reactions

Christensen *et al.*⁴⁰ have observed the ^{14}C group from the $^{58}\text{Ni}(^{16}\text{O}, ^{14}\text{C})$ reaction although for somewhat higher ^{16}O energies (60 MeV) than used in the present study. Using the 1332.5-keV γ ray in ^{60}Ni as a signature of the two-nucleon transfer reactions, we deduced the limits given in Table I. Absence of this same γ ray in the in-beam spectrum led to an upper limit for the $^{58}\text{Ni}(^{16}\text{O}, ^{14}\text{O})$ reaction.

There is weak evidence for ^{59}Cu which would be produced in the $^{58}\text{Ni}(^{16}\text{O}, ^{15}\text{N})$ reaction, namely a 1302-keV γ ray observed in one set of our short irradiations. This is the energy of the strongest γ ray in the decay of 82-sec ^{59}Cu .⁴¹ The cross sections given in Table I assume this is the correct interpretation. The cross section for $E_{^{16}\text{O}} = 46$ MeV (average energy in the target is 44.1 MeV) appears reasonable when compared with the recent work of Korner *et al.*⁴² on the $^{62}, ^{64}\text{Ni}(^{16}\text{O}, ^{15}\text{N})$ reactions. An integration of their differential cross sections for the two strongest groups in each of these two

reactions at $E_{^{16}\text{O}} = 48$ MeV gave ≈ 7 and 12 mb.

The lack of a 1377.6-keV γ ray from the decay of 36-h ^{57}Ni and of an in-beam 878-keV γ ray were used, respectively, to put limits on the cross sections for the $^{58}\text{Ni}(^{16}\text{O}, ^{17}\text{O})$ and $(^{16}\text{O}, ^{15}\text{O})$ reactions.

APPENDIX B. $^{60}\text{Ni}(^{16}\text{O}, X)$ reactions

A. $^{60}\text{Ni}(^{16}\text{O}, x)$ reactions

The identification of these reactions was based on observation of two γ rays consistent with the decay of ^{75}Br to ^{75}Se . Their energies and relative intensities are 286.8 ± 0.7 keV (100) and 140 ± 1 keV (6 ± 3) which are in good agreement with properties of the two strongest lines reported by Ray *et al.*⁴³ and by Ladenbauer-Bellis and Bakhru.⁴⁴ The half-life of 1.78 ± 0.15 h which could only be obtained from the stronger transition compares favorably with 1.68 h given in these two references. A 428-keV γ ray which has the energy of a ^{75}Se γ ray was observed but was too strong and had a $T_{1/2} > 2.5$ h. γ rays from the decay of 120-day ^{75}Se should also be present but because of the long half-life their calculated yields were less than our limit of observability.

Differentiation between the $^{60}\text{Ni}(^{16}\text{O}, n)^{75}\text{Kr}$ and $(^{16}\text{O}, p)^{75}\text{Br}$ reactions requires identification of γ rays from the decay of ^{75}Kr . All that is known about ^{75}Kr is energies of two of its γ rays,⁴⁵ 133 and 157 keV, and its $T_{1/2}$ of 5.5 min. We do see a 133-keV γ ray with $T_{1/2} < 4$ min in the 46-MeV ^{16}O -induced spectrum. If this is a γ ray in ^{75}Br and all of the ^{75}Kr decay passes through this transition, the cross section of the $^{60}\text{Ni}(^{16}\text{O}, n)^{75}\text{Kr}$ reaction for 46-MeV ^{16}O projectiles is 0.2 mb.

B. $^{60}\text{Ni}(^{16}\text{O}, 2x)$ reactions

Since no γ rays from the decay of ^{74}Kr are known and since ^{74}Se is stable, cross sections of the $^{60}\text{Ni}(^{16}\text{O}, 2n)^{74}\text{Kr}$ and $^{60}\text{Ni}(^{16}\text{O}, 2p)^{74}\text{Se}$ were deduced from the in-beam γ -ray spectra. A γ ray was observed at 429 keV which according to Nolte *et al.*⁷ is the energy of the $2 \rightarrow 0$ transition in ^{74}Kr . Stronger γ rays of ^{74}Se were seen at 966 ($8^+ - 6^+$), 864 ($6^+ - 4^+$), 728 ($4^+ - 2^+$), and 633 keV ($2^+ - 0^+$) in agreement with those given by Lieder and Draper²⁸ in their (α, xn) studies.

The majority of γ rays observed when ^{60}Ni was bombarded with ^{16}O ions has a half-life consistent with the decay of ^{74}Br to ^{74}Se . More than 30 of the stronger ones have energies and relative intensities in excellent agreement with those given by Goring and Hartrott.⁴⁶ Like the intensities of Goring and Hartrott, ours are frequently significantly different from those given by Ladenbauer-

Bellis and Bakhru.⁴⁷

Additional γ -ray peaks were observed which were not reported by Goring and Hartrott⁴⁶ and yet have half-lives compatible with that of 40-min ^{74}Br . Because their intensities are generally smaller than the weakest ones listed by Goring and Hartrott, we suggest they are due to ^{74}Br but were below their limit of observability. They are listed in Table IV. Several of these lines have energies consistent with those given for ^{74}Se transitions by Ladenbauer-Bellis and Bakhru⁴⁷ as having intensities less than 1% of the 635-keV γ ray.

The relative intensity for decay of ^{74}Br to the ground state of ^{74}Se has not been previously reported. However, it was deduced as 0.19 ± 0.10 of the total decay by comparing the sum of the cross sections for the neutron-emitting reactions ($^{16}\text{O}, 2n$), ($^{16}\text{O}, pn$), ($^{16}\text{O}, \alpha n$), and ($^{16}\text{O}, 2pn$) as a function of projectile energy to that found by Bair

TABLE IV. Additional γ rays which are suggested by their half-life as attributable to the decay of ^{74}Br . Their intensities are normalized to 117 for that of the two γ rays at 634.8 keV.

E_γ (keV) ^a	I_γ	$T_{1/2}$ (h)
979.7	0.40 ± 0.30	$1.3^{+3}_{-0.6}$
1022.9	0.92 ± 0.15	0.8 ± 0.2
1145.8	0.56 ± 0.10	0.9 ± 0.2
1204.0	0.8 ± 0.4	$0.7^{+0.5}_{-0.2}$
1261.7	0.6 ± 0.3	> 0.4
1289.3	0.5 ± 0.2	$0.7^{+0.5}_{-0.2}$
1460.3	1.8 ± 0.2	0.8 ± 0.1
1468.3	1.1 ± 0.2	0.9 ± 0.2
1508.3	0.30 ± 0.15	$1.0^{+2.6}_{-0.3}$
1514.7	0.45 ± 0.20	$0.9^{+2.2}_{-0.5}$
1555.3	0.32 ± 0.19	$0.6^{+1.0}_{-0.4}$
1566.2	0.38 ± 0.15	< 0.9
1853.8	0.8 ± 0.2	$0.5^{+0.4}_{-0.2}$
1933.2	0.44 ± 0.20	$1.0^{+3}_{-0.3}$
1995.2	0.56 ± 0.15	$1.1^{+1.8}_{-0.8}$
2098.5	0.53 ± 0.19	$0.6^{+1.0}_{-0.3}$
2115.2	0.39 ± 0.16	$0.4^{+0.7}_{-0.2}$
2131.4	0.83 ± 0.12	0.72 ± 0.2
2150.7 ^b	0.8 ± 0.2	$0.6^{+0.7}_{-0.2}$
2158.2	0.5 ± 0.2	$0.9^{+1.2}_{-0.4}$
2167.4	0.7 ± 0.2	$1.0^{+0.9}_{-0.4}$
2207.4 ^b	0.6 ± 0.2	$0.7^{+0.8}_{-0.3}$
2216.7	0.6 ± 0.2	$1.2^{+5.5}_{-0.6}$
2228.6	0.29 ± 0.15	$0.9^{+0.6}_{-0.4}$
2276.2	0.7 ± 0.2	$1.0^{+1.0}_{-0.3}$
2370.7	0.75 ± 0.20	$0.8^{+0.5}_{-0.3}$
2445.0	0.5 ± 0.2	$0.8^{+0.7}_{-0.2}$
2471.3	0.8 ± 0.2	$0.7^{+0.5}_{-0.3}$
2484.1	0.85 ± 0.20	$0.7^{+0.3}_{-0.2}$

^a The uncertainty in energy is ± 0.8 keV.

^b Attributed to a double-escape peak in Ref. 47.

*et al.*⁸ for emission of all neutrons when ^{60}Ni was bombarded with ^{16}O ions. Comparison of the two measurements with a 19% ground-state branch for decay of ^{74}Br to ^{74}Se included is illustrated in Fig. 14.

The radioactivity ^{74}Kr has a $T_{1/2}$ of 16 min,⁴⁸ but there is no reported γ ray. The only unexplained γ ray with comparable half-life in this work is at 203.6 keV ($T_{1/2} = 10^{+10}_{-4}$ min). It would give the $^{60}\text{Ni}(^{16}\text{O}, 2n)$ cross sections extracted from the in-beam spectra if $\sim 7\%$ of the total decay of ^{74}Kr is via this transition.

C. $^{60}\text{Ni}(^{16}\text{O}, 3x)$ reactions

The radioactivity ^{73}Se which could result from the $^{60}\text{Ni}(^{16}\text{O}, p2n)$ and $(^{16}\text{O}, 2pn)$ reactions (the $3n$ channel is energetically impossible) was indicated by the 361.0-keV γ ray with $T_{1/2}$ of 7.8 ± 0.7 h. This is to be compared with the strongest transition in the decay of 7.2-h ^{73}Se at 361.1 keV.²¹ A strong transition at 67 keV is below our spectral energy threshold. The other known γ rays are below the sensitivity of our measurement.

No γ ray was observed from the 42-min isomer of ^{73}Se . (the limit on its cross section is included

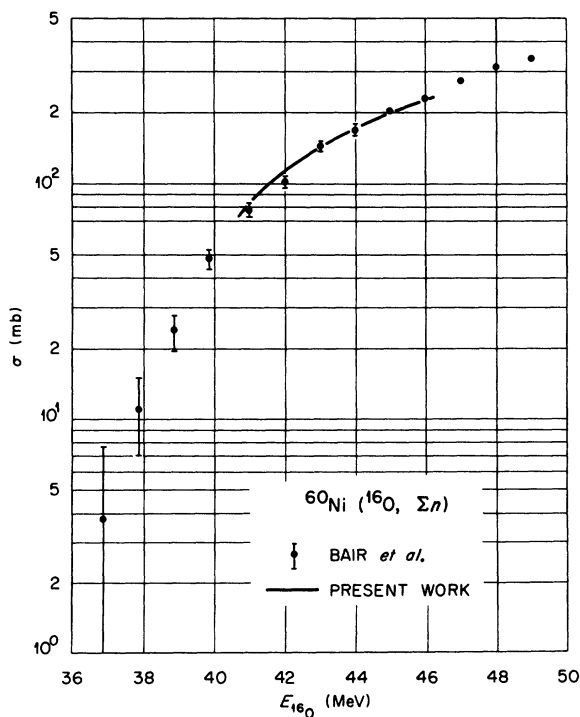


FIG. 14. Cross section for neutron emission obtained by Bair *et al.* (Ref. 8) and in the present work for ^{16}O irradiation of ^{60}Ni . The solid curve is extracted from the present γ -ray studies if the decay of ^{74}Br to the ground state of ^{74}Se is 19% of its total decay.

in Table II), nor were γ rays from the decay of 3.3-min ^{73}Br (Ref. 23) observed which would result from the $^{60}\text{Ni}(^{16}\text{O}, p2n)$ reaction, and thus only a limit can be placed on its cross section.

D. $^{60}\text{Ni}(^{16}\text{O}, \alpha)$ reaction

Because the half-life of the residual nucleus ^{72}Se is long ($T_{1/2} = 8.5$ day) the resulting γ -ray yield would be low. Thus, the lowest limit (as given in Table II) was obtained from in-beam γ -ray spectra.

E. $^{60}\text{Ni}(^{16}\text{O}, \alpha n)$ reaction

The $^{60}\text{Ni}(^{16}\text{O}, \alpha n)$ reaction was established from the stronger γ rays from the decay of ^{71}Se (Ref. 29) seen at 148 ± 1 , 830.5 ± 0.7 , 1094.8 ± 0.7 , and 1242 ± 1 keV. Then the sum of the cross sections for the $^{60}\text{Ni}(^{16}\text{O}, \alpha n)$ and $(^{16}\text{O}, \alpha p)$ reactions came from the γ rays due to the decay of $^{71}\text{As} \rightarrow ^{71}\text{Ge}$ as based on γ rays with energies of 174.7 ± 0.8 , 327.0 ± 1.0 , 500.0 ± 1.0 , and 1095.7 ± 0.6 keV.

F. $^{60}\text{Ni}(^{16}\text{O}, 2\alpha)$ reaction

Since the 2α channel was observed with the ^{58}Ni target, a search was made for the γ rays from the double decay of 287-day $^{68}\text{Ge} \rightarrow 68\text{-min } ^{68}\text{Ga} \rightarrow ^{68}\text{Zn}$; but the long half-life of ^{68}Ge prevented determination of any sensible cross-section limit. If the levels of ^{68}Ge were known the cross section might be attainable from in-beam γ -ray spectra.

G. $^{60}\text{Ni}(^{16}\text{O}, ^{12}\text{C})$ reaction

This results in the stable nucleus ^{64}Zn . A γ ray of appropriate energy for the $2 \rightarrow 0$ transition of ^{64}Zn was not resolvable from the continuum in the in-beam γ -ray spectra and thus only a cross-section limit was obtainable.

H. One- and two-nucleon transfer reactions

There are two γ rays of appropriate characteristics to indicate the presence of ^{61}Cu which results from the $^{60}\text{Ni}(^{16}\text{O}, ^{15}\text{N})$ reaction. Their energies (and relative intensities) of 283.4 ± 1.0 keV (99 ± 33) and 656.2 ± 0.6 (100) are to be compared with 283.7 ± 0.2 keV (113 ± 8) and 656.0 ± 0.2 (100) as reported by Ritter and Larson.⁴⁹ Otherwise only cross-section limits were obtainable for these nucleon-transfer reactions. Except for that of the $^{60}\text{Ni}(^{16}\text{O}, ^{14}\text{N})^{62}\text{Cu}$ reaction, these are given in Table II for $E_{^{16}\text{O}} = 46$ MeV. Because ^{62}Cu decays predominantly to the ground state of ^{62}Ni (Ref. 50) only a poor limit of 140 mb can be extracted for the $(^{16}\text{O}, ^{14}\text{N})$ reaction cross section.

- *Work sponsored by the U.S. Atomic Energy Commission under contract with Union Carbide Corporation.
- ¹F. S. Stephens, J. R. Leigh, and R. M. Diamond, Nucl. Phys. A170, 321 (1970).
 - ²T. D. Thomas, Annu. Rev. Nucl. Sci. 18, 343 (1968).
 - ³M. Blann, Phys. Rev. 157, 860 (1967); and in Proceedings of the Heavy Ion Summer Study, edited by S. T. Thornton (U. S. Atomic Energy Commission Technical Information Center, Oak Ridge, Tenn., 1972), CONF-720669, p. 269.
 - ⁴Preliminary results of these measurements were given in J. Phys. (Paris) Suppl. No. 11-12, 32, 265 (1971).
 - ⁵E. Collins, J. H. Hamilton, R. L. Robinson, H. J. Kim, and J. L. C. Ford, Jr., Bull. Am. Phys. Soc. 17, 560 (1972); and to be published.
 - ⁶T. A. Doron and M. Blann, Nucl. Phys. A161, 12 (1971).
 - ⁷E. Nolte, W. Kutschera, Y. Shida, and H. Morinaga, Phys. Lett. 33B, 294 (1970).
 - ⁸J. K. Bair, W. B. Dress, C. H. Johnson, and P. H. Stelson, private communication; and Bull. Am. Phys. Soc. 17, 530 (1972).
 - ⁹F. G. Perey, private communication.
 - ¹⁰A. W. Obst, D. L. McShan, and R. H. Davis, Phys. Rev. C 6, 1814 (1972).
 - ¹¹P. R. Christensen, I. Chernov, E. E. Gross, R. Stokstad, and F. Videbaek, Nucl. Phys. A207, 433 (1973).
 - ¹²Y. LeBeyec, M. Lefort, and A. Vigny, Phys. Rev. C 3, 1268 (1971).
 - ¹³H. Gauvin, Y. LeBeyec, M. Lefort, and C. Deprun, Phys. Rev. Lett. 28, 697 (1972).
 - ¹⁴W. R. Smith, Comp. Phys. Commun. 1, 106 (1969).
 - ¹⁵P. Boschung, J. T. Lindow, and E. F. Shrader, Nucl. Phys. A161, 593 (1971).
 - ¹⁶C. M. Perey, F. G. Perey, J. K. Dickens, and R. J. Silva, Phys. Rev. 175, 1460 (1968).
 - ¹⁷R. M. Eisberg and C. E. Porter, Rev. Mod. Phys. 33, 190 (1961).
 - ¹⁸A. H. Wapstra and N. B. Gove, Nucl. Data A9, 267 (1971).
 - ¹⁹N. B. Gove and A. H. Wapstra, Nucl. Data A11, 128 (1972).
 - ²⁰M. Blann, private communication.
 - ²¹K. W. Marlow and A. Faas, Nucl. Phys. A132, 339 (1969).
 - ²²R. D. Meeker and A. B. Tucker, Nucl. Phys. A157, 337 (1970).
 - ²³G. Murray, W. J. K. White, J. C. Willmott, and R. F. Entwistle, Nucl. Phys. A142, 21 (1970).
 - ²⁴C. N. Davids and D. R. Goosman, Phys. Rev. C 8, 1029 (1973).
 - ²⁵C. N. Davids and D. R. Goosman, Bull. Am. Phys. Soc. 18, 720 (1973).
 - ²⁶H. Schmeing, J. C. Hardy, R. L. Graham, and J. S. Geiger, Bull. Am. Phys. Soc. 18, 720 (1973); and private communication.
 - ²⁷D. C. Camp, Nucl. Phys. A121, 561 (1968).
 - ²⁸R. M. Leider and J. E. Draper, Phys. Rev. C 2, 531 (1970).
 - ²⁹U. F. v. Hundelshauen, Z. Phys. 225, 125 (1969).
 - ³⁰G. Murray, N. E. Sanderson, and J. C. Willmott, Nucl. Phys. A171, 435 (1971).
 - ³¹A. P. DeRuiter, H. Verheul, and J. Konijn, Nucl. Phys. A116, 473 (1968).
 - ³²S. C. Pancholi and S. Raman, Nucl. Data B2 (No. 6), 111 (1968).
 - ³³S. Muzynski and S. K. Mark, Nucl. Phys. A142, 459 (1970).
 - ³⁴A. N. Bilge and G. G. J. Boswell, J. Inorg. Nucl. Chem. 34, 407 (1972).
 - ³⁵F. W. N. de Boer, E. W. A. Lingeman, R. van Lieshout, and R. A. Ricci, Nucl. Phys. A158, 166 (1970).
 - ³⁶M. J. Martin and M. N. Rao, Nucl. Data B2 (No. 6), 43 (1968).
 - ³⁷G. H. Dulfer, T. J. Ketel, V. A. Van Rooijen, M. E. J. Wigmans, and H. Verheul, Nucl. Phys. A182, 433 (1972).
 - ³⁸E. J. Hoffman and D. G. Sarantites, Phys. Rev. 177, 1640 (1969).
 - ³⁹D. M. Van Patter, D. Neuffer, H. L. Scott, and C. Moazed, Nucl. Phys. A146, 427 (1970).
 - ⁴⁰P. R. Christensen, V. I. Manko, F. D. Becchetti, and R. J. Nickles, Nucl. Phys. A207, 33 (1973).
 - ⁴¹J. Vervier, Nucl. Data B2 (No. 5), 1 (1968).
 - ⁴²H. J. Korner, G. C. Morrison, L. R. Greenwood, and R. H. Siemssen, Phys. Rev. C 7, 107 (1973).
 - ⁴³S. Ray, J. N. Mo, S. Muszynski, and S. K. Mark, Nucl. Phys. A138, 49 (1969).
 - ⁴⁴I. Ladenbauer-Bellis and H. Bakhru, Phys. Rev. 178, 2019 (1969).
 - ⁴⁵ISOLDE collaborators, Phys. Lett. 28B, 415 (1969).
 - ⁴⁶S. Goring and M. V. Hartrott, Nucl. Phys. A152, 241 (1970).
 - ⁴⁷I. Ladenbauer-Bellis and H. Bakhru, Phys. Rev. 180, 1015 (1969).
 - ⁴⁸W. B. Ewbank, M. J. Martin, S. C. Pancholi, and K. Way, Nucl. Data B1 (No. 6), 59 (1966).
 - ⁴⁹J. C. Ritter and R. E. Larson, Nucl. Phys. A127, 399 (1969).
 - ⁵⁰H. Verheul, Nucl. Data B2 (No. 3), 1 (1967).